

ORIGINAL ARTICLE

Open Access



Mesoporous TiO₂ Nanofiber as Highly Efficient Sulfur Host for Advanced Lithium–Sulfur Batteries

Xinyu Shan¹, Zuoxing Guo¹, Xu Zhang², Jie Yang² and Lianfeng Duan^{2*}

Abstract

Currently, lithium–sulfur batteries suffer from several critical limitations that hinder their practical application, such as the large volumetric expansion of electrode, poor conductivity and lower sulfur utilization. In this work, TiO₂ nanofibers with mesoporous structure have been synthesized by electrospinning and heat treating. As the host material of cathode for Li–S battery, the as prepared samples with novelty structure could enhance the conductivity of cathode composite, promote the utilization of sulfur, and relieve volume expansion for improving the electrochemical property. The initial discharge capacity of TiO₂/S composite cathode is 703 mAh/g and the capacity remained at 652 mAh/g after 200 cycles at 0.1 C, whose the capacity retention remains is at 92.7%, demonstrating great prospect for application in high-performance Li–S batteries.

Keywords: TiO₂ nanofibers, Mesoporous structure, Lithium–sulfur batteries, Cathode, Electrochemical property

1 Introduction

With the rapid development of portable equipment, handheld electronic products and hybrid electric vehicles, problems related to energy storage and conversion devices have attracted more and more attention. Because of low cost of sulfur, no harmful to the environment and higher theoretical energy density, lithium–sulfur batteries are being expected to become the most potential next generation of batteries in the world [1, 2]. However, currently most traditional lithium–sulfur batteries suffer from several critical limitations that hinder their practical application on account of the large volumetric expansion of elemental sulfur during lithiation, poor conductivity of both the final products, and so on. In addition to this, in the discharge process, the major obstacle is that intermediate polysulfides are highly dissolved in organic electrolyte, which the so-called “shuttle effect” causes an irreversible loss of active sulfur, poor cycle stability and

low coulombic efficiency during charge/discharge cycling [3–5].

To overcome these impediments for the development of Li–S batteries, several strategies have been developed. For example, carbon acted as the sulfur matrix (graphene, carbon nanotubes and porous carbon [6–9], which mainly encapsulated the sulfur and polysulfide species into porous conductive materials through physical interaction. Meanwhile, more and more metal oxides as host materials for Li–S batteries has been put forward, owing to their strong chemisorption effect towards polysulfides (LiPSs), including SiO₂, MnO₂, TiO_x, Al₂O₃, etc [10–14]. Among them, titanium dioxide (TiO₂) has drawn much attention due to its low cost, environmental protection and structural stability [15]. An et al. [16] prepared TiO₂@NC interlayer to absorb polysulfide in Li–S batteries. Because of good electronic conductivity, the reversible capacity reached 1460 mAh/g at 0.2 C. She et al. [17] designed a sulphur-TiO₂ yolk-shell nano-architecture to take in the large volumetric expansion of sulphur and minimize polysulfide dissolution, and the capacity decayed 0.033% every cycle after 1000 cycles. Li et al. [18] designed mesoporous hollow TiO₂ spheres (HTSs) to solve the

*Correspondence: duanlf@ccut.edu.cn

² Advanced Institute of Materials Science & Department of Materials Science and Engineering, Changchun University of Technology, Changchun 130012, China

Full list of author information is available at the end of the article

above problems, and the capacity retention of 71% at 1 C (1 C = 1672 mA/g). The mesoporous morphologies of host is important for the improving the electrochemical property of Li-S batteries, because of the higher utilization of sulfur and chemisorption of lithium polysulfides. Moreover, it could afford large surface to infuse sulfur and accommodate volume changes during the charge/discharge reactions. Therefore, it is important to prepare the TiO_2 with the mesoporous structure by simple methods and research on charge and discharge mechanism of Li-S batteries deeply.

Herein, the mesoporous TiO_2 nanofibers were synthesized through an electrospinning method and subsequent thermal treatment. The mesoporous structure could encapsulate sulfur in their pores to trap soluble polysulfides (S_8 combining with the Li^+ in the anode), and accommodate large volumetric expansion of sulphur during lithiation/delithiation. In addition, the cathode conductivity is improved by TiO_2/S composite as electrodes. It results in excellent electrochemical performance and significantly improved cycle stability of the TiO_2/S composite cathode for Li-S batteries.

2 Experimental Section

2.1 RepARATION of the Porous Nanofiber TiO_2 Membranes

The nanofiber TiO_2 was prepared by electrospinning, the details as follows: 0.8 g Polyvinylpyrrolidone (PVP) was directly dissolved in 6 mL ethanol, and stirred for 3 h. Meanwhile, to obtain a solution of TiO_2 , 2.5 mL tetra-n-butyl titanate was dissolved in 2 mL acetic acid and 5 mL ethanol, and stirred for 3 h. After that above mixture was mixed with the PVP/ethanol solution together, and stirring for 12 h at room temperature. This solution was loaded into a perfusion tube equipped with pipette tip through syringe with silver-coated needle. The pipette tip was connected to a high-voltage power supply. The electric voltage was set as 15 kV. Gained nonwoven fabrics was consist of PVP/ TiO_2 nanofibers. After peeled off, nonwoven fabrics was calcined at 500 °C with heat-up speed of 5 °C/min for 2 h in air flow, following by being calcined at 700 °C for 5 h to yield the final products.

2.2 Preparation of TiO_2/S Cathode

As-prepared Nanofiber TiO_2 and sulfur powder in a mass ratio of 3:7 were mixed and ground together for 30 min. Then the mixture of powder was converted to a sealed stainless steel vessel and calcined for 24 h at 155 °C. Finally, TiO_2/S cathode was obtained, corresponding to a sulfur loading of 3.0 mg/cm² and a sulfur content of 70 wt% in the whole cathode.

2.3 Materials Characterization

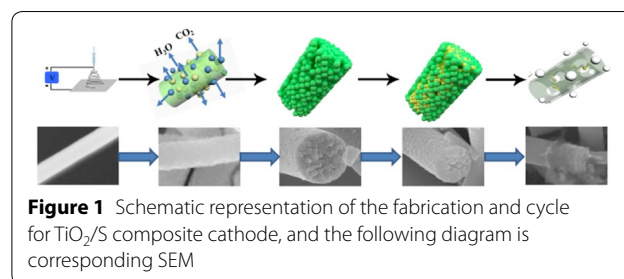
The microstructure of the samples were investigated by X-ray diffraction (XRD, D-MAX II A X-ray diffractometer). The micro morphological images were obtained by field emission scanning electron microscope (FE-SEM, S4800, Hitachi) and transmission electron microscopy (TEM, Tecnai F20). Energy-dispersive X-ray spectroscopy (EDS) was measured to gain the elemental mapping results. Thermogravimetric (TG) analysis (Perkin-Elmer TGA 7 thermogravimetric analyzer) was used to evaluate the sulfur content of TiO_2/S cathode at a heating rate of 5 °C/min from 40 °C to 600 °C in flowing N_2 . The pore size distributions and specific surface area of TiO_2/S cathode were measured by TriStar II 3020 3.02 (Micromeritics Instrument Corporation, USA).

2.4 Electrochemical Performance Measurements

CR2025 coin cells were prepared in a glove box, which is filled with argon and conducted electrochemical testings. The working cathode was fabricated by coating a mixture containing 10 wt% polyvinylidene fluoride (PVDF) as a binder dissolved in NMP, 10 wt% carbon black and 80 wt% active material (nanofiber TiO_2/S) on an aluminum foil following by drying at 60 °C for 12 h. Then the electrode disks were punched. Li metal was used as the anode. The electrolyte was a solution of 1.0 M LiTFSI dissolved in a mixture of dioxolane (DOL) (99.8%, Sigma-Aldrich) and 1,2-dimethoxyethane (DME) (99.5, Sigma-Aldrich) (1:1 by volume) with LiNO_3 (1 wt%) additive. Separator (Celgard 2400) was bought from Celgard Company. CR2025 coin cells were assembled in an argon filled glovebox with water and oxygen content kept below 0.1 ppm and used for electrochemical tests. Galvanostatic charge/discharge cycling was carried out using a LAND-CT2001A instrument (Wuhan, China) in the voltage range 1.5 to 3 V.

3 Results and Discussion

Figure 1 shows the fabrication and electrochemical process of TiO_2/S composite as cathode for Li-S battery. In step 1, the smooth of TiO_2/PVP nanofibers was fabricated by electrospinning. Followed by pyrolysis of PVP, which is pyrolyzed into CO_2 and H_2O at high



temperature calcination in Air-flow, the TiO_2 nanofibers with mesoporous structure could be gained. In step 4, the TiO_2 infused with sulfur forming the TiO_2/S cathode. The sulfur elements are uniformly distributed in the TiO_2 nanofibers because of the mesoporous structure and polar metal-O bond. After testing for 200 cycles, clear and smooth surface of TiO_2/S composite electrode can be observed from the typical SEM images (in step 5), which improving the electrochemical performance.

The SEM images of the synthesis PVP/ TiO_2 composite nanofiber by electrospinning are shown in Figure 2. Figure 2(a) shows a typical low-magnification SEM image of PVP/ TiO_2 composite fibers (the average diameter is about 200 nm). The high-magnification SEM image of the composite nanofibers with smooth surface (Figure 2(b)). After electrospinning, the composite nanofibers were calcined to obtain pure TiO_2 nanofibers. From the Figure 2(c) and (d), the TiO_2 nanofibers with the average diameters about 200 nm were synthesized. Cross sections of enlarged TiO_2 nanofibers in Figure 2(d) clearly shows that the fibers are very rough with many wormhole-like pores which could be used as good sulfur host to infuse high content of sulfur.

After preparing of TiO_2/S , the morphology of the TiO_2 nanofibers as the host could not be changed after the infusion of sulfur (as shown in Figure 3(a) and (b)). The TEM images of TiO_2 nanofibers before and after infusion of sulfur are shown in Figure 3(c), (d). The mesoporous structure can be clearly seen in the TEM image of TiO_2 nanofibers, these porous structure was disappeared in the TEM image of TiO_2/S nanofibers, reflecting the good infusion of sulfur by mesoporous structure in TiO_2

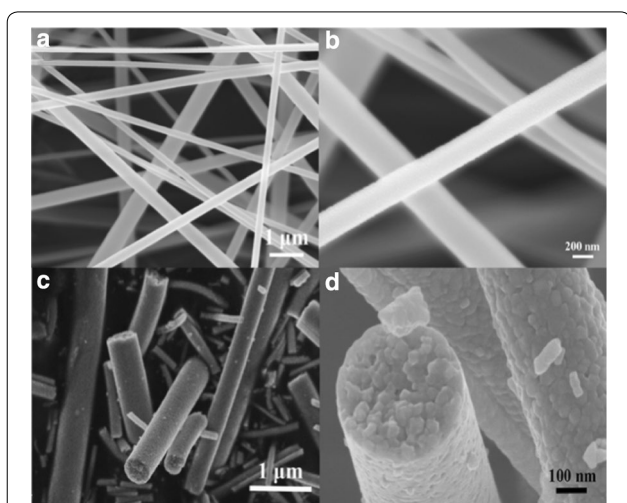


Figure 2 SEM images of the as-spun PVP/ TiO_2 composite nanofibers: **a** the lower magnification and **b** the higher magnification, and after calcination the TiO_2 nanofibers: **c** the lower magnification and **d** the higher magnification

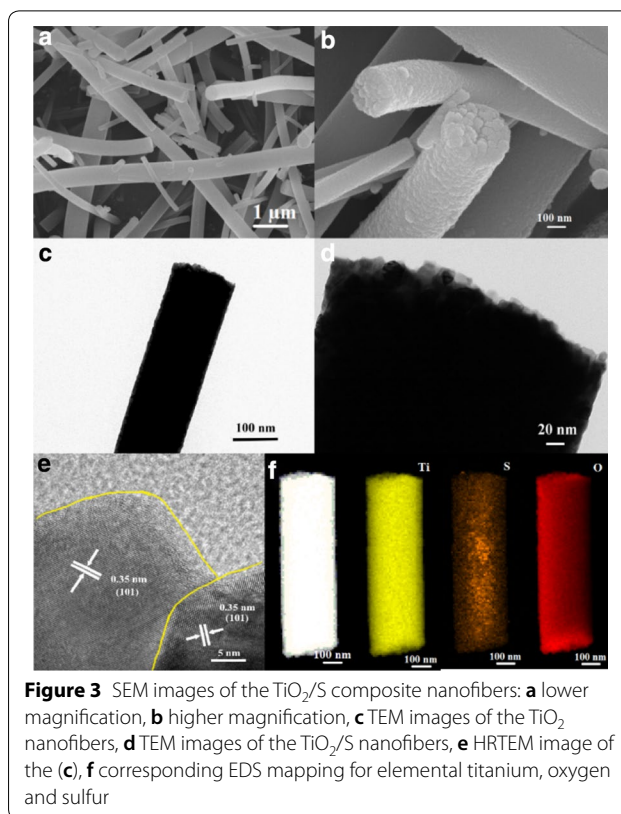


Figure 3 SEM images of the TiO_2/S composite nanofibers: **a** lower magnification, **b** higher magnification, **c** TEM images of the TiO_2 nanofibers, **d** TEM images of the TiO_2/S nanofibers, **e** HRTEM image of the (c), **f** corresponding EDS mapping for elemental titanium, oxygen and sulfur

nanofibers. The HRTEM image (Figure 3(e)) reveals the clear lattice fringe spacing is 0.35 nm, which is consistent with the (101) crystalline interplanar spacing of TiO_2 structure. Additionally EDS area mapping showing in Figure 3(f), and can see the elemental of Ti, O, and S homogeneous distribution in all over the fiber.

The XRD patterns of TiO_2 and TiO_2/S nanofibers are shown in Figure 4 to confirm the crystal phase formation about synthesized TiO_2 nanofibers and the existence of sulfur about TiO_2/S nanofibers. The XRD pattern of TiO_2 nanofibers demonstrates that TiO_2 possesses almost pure rutile (JCPDS No. 65-0191) structure [19, 20]. Then, the XRD pattern of TiO_2/S composites was well defined for orthorhombic structure of crystalline sulfur (JCPDS Card No. 08-0247), which is identical to the element sulfur powder [5, 21]. It reveals the TiO_2 nanofibers with sulfur loading have been synthesized successfully.

The nitrogen adsorption and desorption isotherms of the TiO_2 and TiO_2/S composite were obtained, which correspond to type IV isotherms in the IUPAC classification with a typical mesopore hysteresis loop, from Figure 5(a) [22, 23]. Notably, compared with TiO_2/S composite, TiO_2 has larger pore volume and specific surface area. The pore size distribution of TiO_2 fibers is in the range of 20–30 nm by Barrett-Joyner-Halenda as shown in Figure 5(a) inset. After sulfur incorporation, the fibers

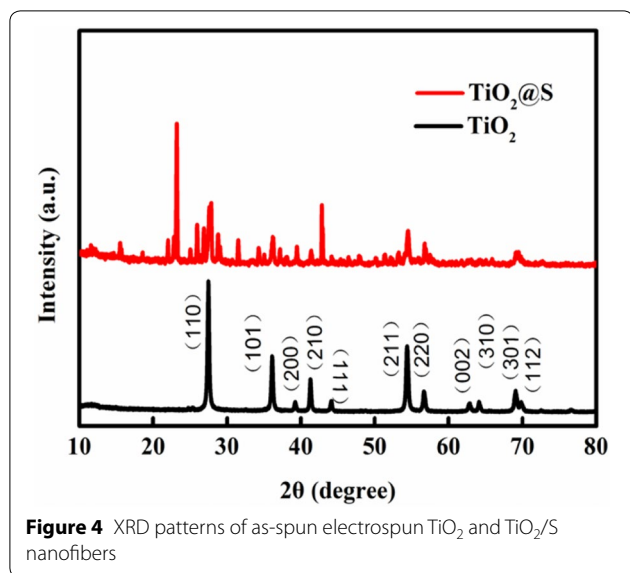


Figure 4 XRD patterns of as-spun electrospun TiO₂ and TiO₂/S nanofibers

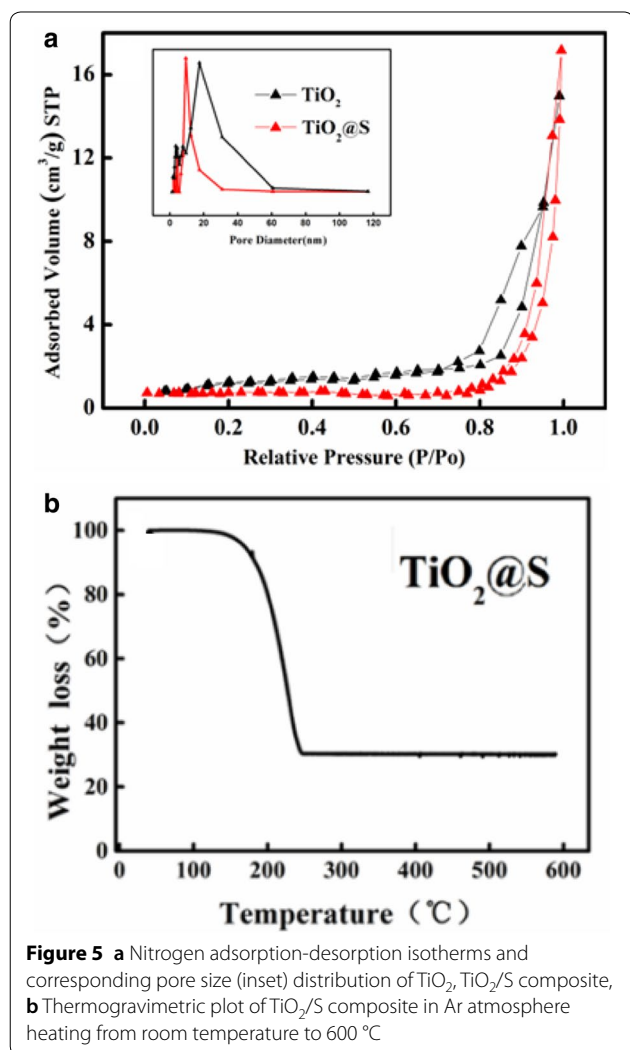


Figure 5 a Nitrogen adsorption-desorption isotherms and corresponding pore size (inset) distribution of TiO₂, TiO₂/S composite, b Thermogravimetric plot of TiO₂/S composite in Ar atmosphere heating from room temperature to 600 °C

pore distribution decrease to 10–20 nm, because S particles is covered on or embedded into the mesopores of TiO₂ fibers. To evaluate the content of sulfur in TiO₂/S composite, thermo gravimetric (TGA) was performed from room temperature to 600 °C at a heating rate of 10 °C/min under N₂ atmosphere. The sulfur content in TiO₂/S nanocomposite (Figure 5(b)) is estimated as high as 70 wt%, which demonstrates such higher sulfur loading.

Figure 6(a) and (b) display the galvanostatic the discharging-charging curves of the TiO₂/S composite electrode at a current rate of 0.2 and 0.5 C (1 C = 1672 mA/g). The profile apparently shows the two plateaus in the discharging curves, which could be assigned to the two-step reaction of sulfur with lithium. The first plateau, at 2.35 V, was due to the reduction of sulfur to higher polysulfide. The low voltage plateau, at 2.1 V, showed the reactions of the higher polysulfides (Li₂S_n, 4 ≤ n ≤ 8) finally the further to the lower polysulfides (Li₂S_n, n ≤ 3) [24–27]. And the initial discharge capacity and charge capacity of as prepared electrode were 763 mAh/g and 827 mAh/g at 0.2 C, respectively. And at 0.5 C as shown in Figure 6(b), the electrode discharge capacities was found to be 423 mAh/g, and charge capacities was 405 mAh/g.

The excellently stable cycling performance of TiO₂/S composite electrodes at different current densities have been shown in Figure 6(c). The TiO₂/S electrodes exhibit the excellent capacity retention at 0.1, 0.2 and 0.5 C. The initial discharge capacity was 703 mAh/g and the capacity remained at 652 mAh/g after 200 cycles at 0.1 C. Figure 6(d) is the discharge rate capability performance with 100 cycles at different current densities. When the current density is increased to 0.2, 0.5 and 1 C, the discharge

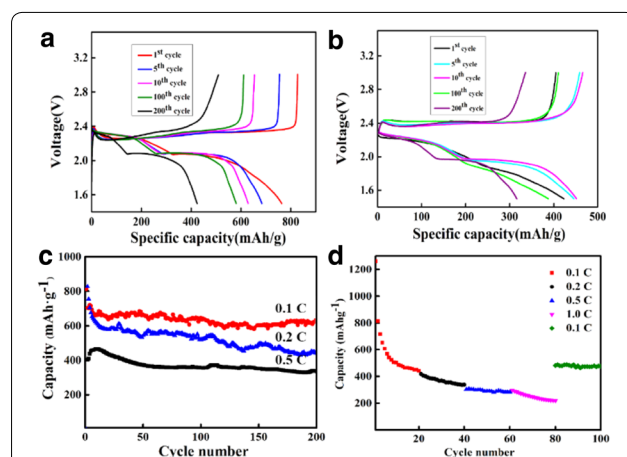


Figure 6 Electrochemical performance of TiO₂/S nanocomposite structures. Galvanostatic charge-discharge voltage profiles of TiO₂/S cathodes between 1.5 and 3.0 V at a 0.2 C, b 0.5 C, c Cycling performance of TiO₂/S cathodes at a current density of 0.1 C, 0.2 C and 0.5 C, d Rate capability of TiO₂/S composite electrodes at various current densities from 0.1, 0.2, 0.5 to 1 C

capacities are 498, 402 and 298 mAh/g. When the current density returns to 0.1 C, the reversible capacity was recovered to 613 mAh/g, indicating the reliability and stability of the TiO₂/S composite electrode.

The SEM images of the TiO₂/S cathode after cycled 200 times are displayed in Figure 7(a). The TiO₂/S fibers are still maintains the original fiber structure, although the some nanowire structure was destroyed. From Figure 7(b)–(d), the cathode elemental of Ti, O, and S still displays homogeneous distribution. It reveals that sulfur could be trapped in the nanofibers after 200 cycles, and further shows the advantages of mesoporous nanofibers in repeated cycling, which accordingly enhances the cyclic stability and rate capability. Figure 7(e) is corresponding reaction mechanism of the TiO₂/S cathode during cycling. In the discharge process, S₈ (elemental sulfur) in the nanofibers is combined with the Li⁺ from the anode, and reduced to form soluble Li₂S_n (2 ≤ n < 8), which is also trapped in the mesoporous structure without diffused into the electrolyte and transferred to anode [28]. Then the soluble Li₂S_n is further reduced

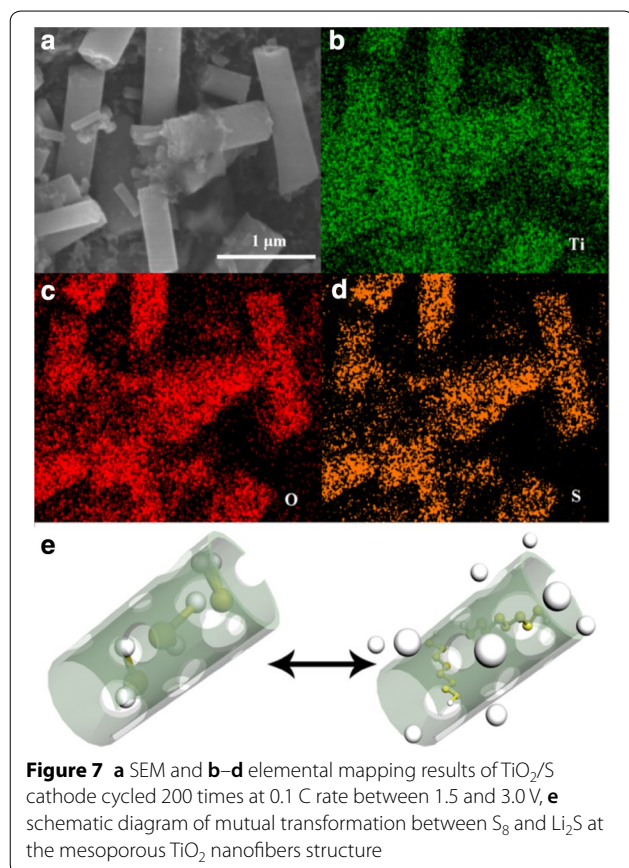


Table 1 Electrochemical performance comparison of TiO₂-S with different morphologies in previously reported

Cathode material	Cycle number	Cycling stability	Ref. No.
TiO ₂ rods/S	50	530 mAh/g (0.2 C)	[5]
TiO ₂ sphere/S	100	371 mAh/g (1.0 C)	[18]
Mesoporous TiO ₂ /S	100	676 mAh/g (0.5 C)	[8]
TiO ₂ sphere/S	100	705 mAh/g (0.5 C)	[27]
TiO ₂ nanofibers /S	200	652 mAh/g (0.1 C)	This work

to insoluble Li₂S. Because the process of elemental sulfur reacted to form lithium polysulfide and eventually to lithium sulfide, which is always carried out in TiO₂ nanofibers, it could prevent the soluble lithium sulfide from being dissolved in the electrolyte, indicating the remission of the “shuttle effects”. Meanwhile, the volume expansion caused by the conversion of sulfur into lithium sulfide could be alleviated, because of TiO₂ nanofibers with mesoporous structure. The electrochemical performance comparison of the TiO₂-S composite between the current work and previously reported in Table 1. It shows that the TiO₂ nanofibers with mesoporous structure in our work improved cycle stability of cathode for Li-S battery.

Therefore, it is owing to the following reasons of TiO₂ nanofiber with mesoporous structure as highly efficient sulfur host for improving cycle stability and high efficiency of battery. Firstly, TiO₂ possesses the excellent catalytic dissociation ability of lithium polysulfides. And rutile phase TiO₂ can in-situ adsorb the lithium polysulfides by stable chemical bonding force leading to further trapping of polysulfide anions [29]. Secondly, the interconnected fiber architecture provided fast pathways for electron/ion transfer and the mesoporous structure provide enough large surface to infuse sulfur while physically absorbing soluble lithium polysulfides and accommodating volume changes by the charge/discharge reactions.

4 Conclusions

TiO₂ nanofibers with mesoporous structure were prepared by post thermal-treatment of electrospun. The fibers as the superior host material to load sulfur up to the 70 wt % for Li-S batteries. The TiO₂/S cathode demonstrated cycle stability and high efficiency. The TiO₂/S cathode maintains a capacity of 652 mAh/g at 0.1 C after 200 cycles, corresponding to a capacity retention of 92.7%. The mesoporous TiO₂ fibers enhance the conductivity of sulfur, promote the utilization of sulfur and provide large active sites to absorb soluble lithium polysulfides. The mesoporous TiO₂ nanofibers as cathode

host material has great potential in high-performance lithium–sulfur batteries.

Authors' Contributions

LD and ZG was in charge of the whole trial; XS wrote the manuscript; XZ and JY assisted with sampling and laboratory analyses. All authors read and approved the final manuscript.

Authors' Information

Xinyu Shan, born in 1996, is currently a master candidate at *Key Laboratory of Automobile Materials, School of Materials Science and Engineering, Jilin University, China*. She received her bachelor degree from *Jilin Jianzhu University, China*, in 2018. Her research interests include solar energy and energy storage materials.

Zuoxing Guo, born in 1963, is currently a professor at *Key Laboratory of Automobile Materials, School of Materials Science and Engineering, Jilin University, China. University, China*, in 2006.

Xu Zhang, born in 1996, is currently a master candidate at *Advanced Institute of Materials Science & Department of Materials Science and Engineering, Changchun University of Technology, China*. She received her bachelor degree from *Changchun University of Technology, China*, in 2017.

Jie Yang, born in 1996, is currently a master candidate at *Advanced Institute of Materials Science & Department of Materials Science and Engineering, Changchun University of Technology, China*. She received her bachelor degree from *Liaocheng University, China*, in 2017.

Lianfeng Duan, born in 1981, is currently a professor at *Advanced Institute of Materials Science & Department of Materials Science and Engineering, Changchun University of Technology, China*, in 2018. He received his PhD degree from *Jilin University, China*, in 2011. His research interests include new energy materials and devices.

Acknowledgements

The authors sincerely thanks to Feifei Zhang of National University of Singapore and Junkai Wang of University of Chinese Academy of Sciences for their critical discussion and reading during manuscript preparation.

Competing Interests

The authors declare that they have no competing interests.

Funding

Supported by National Nature Science Foundation of China (Grant No. 61774022) and Education Department of Jilin Province of China (Grant No. JJKH20181030KJ).

Author Details

¹ Key Laboratory of Automobile Materials, School of Materials Science and Engineering, Jilin University, Changchun 130025, China. ² Advanced Institute of Materials Science & Department of Materials Science and Engineering, Changchun University of Technology, Changchun 130012, China.

Received: 25 May 2019 Revised: 20 June 2019 Accepted: 1 July 2019

Published online: 17 July 2019

References

- [1] X L He, H Hou, X Yuan, et al. Electrocatalytic activity of lithium polysulfides adsorbed into porous TiO₂ coated MWCNTs hybrid structure for lithium–sulfur batteries. *Scientific Reports*, 2017, 7: 40679–40687.
- [2] C L Wang, K Li, F F Zhang, et al. Insight of enhanced redox chemistry for porous MoO₂ carbon-derived framework as polysulfide reservoir in lithium–sulfur batteries. *ACS Appl. Mater. Interfaces*, 2018, 10: 42286–42293.
- [3] G M Liang, J X Wu, X Y Qin, et al. Ultrafine TiO₂ decorated carbon nanofibers as multifunctional interlayer for high performance lithium–sulfur battery. *ACS Appl. Mater. Interfaces*, 2016, 8: 23105–23113.
- [4] R P Fang, S Y Zhao, S F Pei, et al. Toward more reliable lithium–sulfur batteries: An all-graphene cathode structure. *ACS Nano*, 2016, 10: 8676–8682.
- [5] X Z Ma, B Jin, H Y Wang, et al. S-TiO₂ composite cathode materials for lithium/sulfur batteries. *J. Electroanal. Chem.*, 2015, 736: 127–131.
- [6] K Mi, Y Jiang, J K Feng, et al. Hierarchical carbon nanotubes with a thick microporous wall and inner channel as efficient scaffolds for lithium–sulfur batteries. *Adv. Funct. Mater.*, 2016, 26: 1571–1579.
- [7] G X Li, J H Sun, W P Hou, et al. Three-dimensional porous carbon composites containing high sulfur nanoparticle content for high-performance lithium–sulfur batteries. *Nat. Commun.*, 2016, 7: 10601.
- [8] B Ding, L Shen, G Xu, et al. Encapsulating sulfur into mesoporous TiO₂ host as a high performance cathode for lithium–sulfur battery. *Electrochimica Acta*, 2013, 107: 78–84.
- [9] F F Zhang, S P Huang, X Wang, et al. Redox-targeted catalysis for vanadium redox-flow batteries. *Nano Energy*, 2018, 52: 292–299.
- [10] K Z Cao, H Q Liu, Y Li, et al. Encapsulating sulfur in δ-MnO₂ at room temperature for Li–S battery cathode. *Energy Storage Materials*, 2017, 9: 78–84.
- [11] H C Wang, C Y Fan, Y P Zeng, et al. Oxygen-deficient titanium dioxide nanosheets as more effective polysulfide reservoirs for lithium–sulfur batteries. *Chem. Eur.*, 2017, 23: 9666–9673.
- [12] X G Han, Y H Xu, X Y Chen, et al. Reactivation of dissolved polysulfides in Li–S batteries based on atomic layer deposition of Al₂O₃ in nanoporous carbon cloth. *Nano Energy*, 2013, 2: 1197–1206.
- [13] H W Zhu, Y K Jing, M Pal, et al. Mesoporous TiO₂@N-doped carbon composite nanospheres synthesized by the direct carbonization of surfactants after sol-gel process for superior lithium storage. *Nanoscale*, 2017, 9: 1539–1546.
- [14] F F Zhang, C L Wang, G Huang, et al. FeS₂@C nanowires derived from organic-inorganic hybrid nanowires for high-rate and long-life lithium-ion batteries. *J. Power Sources*, 2016, 328: 56–64.
- [15] G G Hu, C Xu, Z H Sun, et al. 3D graphene-foam-reduced-graphene-oxide hybrid nested hierarchical networks for high-performance Li–S batteries. *Adv. Mater.*, 2016, 28: 1603–1609.
- [16] Y L An, Z Zhang, H F Fei, et al. Ultrafine TiO₂ confined in porous-nitrogen-doped carbon from metal-organic frameworks for high-performance lithium sulfur batteries. *ACS Appl. Mater. Interfaces*, 2017, 9: 12400–12407.
- [17] Z W Seh, W Y Li, J J Cha, et al. Sulphur-TiO₂ yolk-shell nanoarchitecture with internal void space for long-cycle lithium–sulphur batteries. *Nat. Commun.*, 2013, 4: 1331.
- [18] J Y Li, B Ding, G Y Xu, et al. Enhanced cycling performance and electrochemical reversibility of a novel sulfur-impregnated mesoporous hollow TiO₂ sphere cathode for advanced Li–S batteries. *Nanoscale*, 2013, 5: 5743–5746.
- [19] J S Cho, Y J Hong, Y C Kang. Electrochemical properties of fiber-in-tube- and filled-structured TiO₂ nanofiber anode materials for lithium-ion batteries. *Chem. Eur.*, 2015, 21: 11082–11087.
- [20] D Zheng, J Xiong, P Guo, et al. Fabrication of improved dye-sensitized solar cells with anatase/rutile TiO₂ nanofibers. *Nanosci. Nanotechnol.*, 2016, 16: 613–618.
- [21] K Mondal, M A Ali, V V Agrawal, et al. Highly sensitive biofunctionalized mesoporous electrospun TiO₂ nanofiber based interface for biosensing. *ACS Appl. Mater. Interfaces*, 2014, 6: 2516–2527.
- [22] Z A Zhang, Q Li, S F Jiang, et al. Sulfur encapsulated in a TiO₂-anchored hollow carbon nanofiber hybrid nanostructure for lithium–sulfur batteries. *Chem. Eur.*, 2015, 21: 1343–1349.
- [23] Y Y Li, Q F Cai, L Wang, et al. Mesoporous TiO₂ nanocrystals/graphene as an efficient sulfur host. *ACS Appl. Mater. Interfaces*, 2016, 8: 23784–23792.
- [24] Z Z Yang, H Y Wang, L Lu, et al. Hierarchical TiO₂ spheres as highly efficient polysulfide host for lithium–sulfur batteries. *Sci. Rep.*, 2016, 6: 22990–22998.
- [25] J Cao, C Chen, Q Zhao, et al. A flexible nanostructured paper of a reduced graphene oxide-sulfur composite for high-performance lithium–sulfur batteries with unconventional configurations. *Adv. Mater.*, 2016, 28: 9629–9636.
- [26] J K Wang, K Q Yue, X D Zhu, et al. C-S@PANI composite with a polymer spherical network structure for high performance lithium–sulfur batteries. *Physical Chemistry Chemical Physics*, 2016, 18: 261–266.
- [27] J Li, J Q Guo, J N Deng, et al. Enhanced electrochemical performance of lithium–sulfur batteries by using mesoporous TiO₂ spheres as host materials for sulfur impregnation. *Materials Letters*, 2017, 189: 188–191.
- [28] Q Zhao, X F Hu, K Zhang, et al. Sulfur nanodots electrodeposited on Ni foam as high-performance cathode for Li–S batteries. *Nano Lett.*, 2015, 15: 721–726.
- [29] G M Zhou, Y B Zhao, C X Zu, et al. Free-standing TiO₂ nanowire-embedded graphene hybrid membrane for advanced Li/dissolved polysulfide batteries. *Nano Energy*, 2015, 12: 240–249.